GSI Annual Report 2009 (extracts)

TASCA

Production and decay of element 114: high cross sections and new nucleus ^{277}Hs ***Page 2***
C. E. Düllmann, D. Ackermann, M. Block, W. Brüchle, H. G. Essel, J. M. Gates, W. Hartmann, F. P. Heßberger, A. Hübner, E. Jäger, J. Khuyagbaatar, B. Kindler, J. Krier, N. Kurz, B. Lommel, M. Schädel, B. Schausten, E. Schimpf, J. Steiner, A. Gorshkov, R. Graeger, A. Türler, A. Yakushev, K. Eberhardt, J. Even, D. Hild, J. V. Kratz, D. Liebe, J. Runke, P. Thörle-Pospiech, N. Wiehl, L.-L. Andersson, R.-D. Herzberg, E. Parr, J. Dvorak, P.A. Ellison, K. E. Gregorich, H. Nitsche, S. Lahiri, M. Maiti, J. P. Omtvedt, A. Semchenkov, D. Rudolph, J. Uusitalo, M. Wegrzecki

The Performance of TASCA in the ^{48}Ca+^{206,207,208}Pb Reactions ***Page 4***
J. Khuyagbaatar, M. Schädel, D. Ackermann, C. E. Düllmann, E. Jäger, F. P. Heßberger, A. Semchenkov, A. Gorshkov, R. Graeger, A. Türler, A. Yakushev, K. Eberhardt, J. Even, J. V. Kratz, L.-L. Andersson, D. Rudolph

TASISpec - Heading towards its first experiment ***Page 5***
L.-L. Andersson, D. Rudolph, D. Ackermann, C. E. Düllmann, K. Eberhardt, J. Even, U. Forsberg, J. Gellanki, J. Gerl, P. Golubev, R. Hoischen, R.-D. Herzberg, F. P. Hessberger, E. Jäger, J. Khuyagbaatar, I. Kojouharov, J. V. Kratz, J. Krier, N. Kurz, E. Merchan, W. Prokopowicz, M. Schädel, H. Schaffner, B. Schausten, E. Schimpf, A. Semchenkov, A. Türler, H.-J. Wollersheim, A. Yakushev, P. Thörle-Pospiech

A new TASCA focal plane detector setup and DAQ system ***Page 6***
A. Gorshkov, J. M. Gates, R. Graeger, A. Türler, A. Yakushev, D. Ackermann, W. Brüchle, C. E. Düllmann, H. G. Essel, E. Jäger, J. Khuyagbaatar, I. Kojouharov, J. Krier, N. Kurz, M. Schädel, B. Schausten, E. Schimpf, J. Dvorak, L.-L. Andersson, D. Rudolph, M. Wegrzecki

COMPACT Coupled to TASCA for Element 114 Chemistry ***Page 7***
A. Yakushev, J.M. Gates, A. Gorshkov, R. Graeger, D. Ackermann, M. Block, W. Brüchle, C. E. Düllmann, H. G. Essel, F. P. Heßberger, A. Hübner, E. Jäger, J. Khuyagbaatar, B. Kindler, J. Krier, N. Kurz, B. Lommel, M. Schädel, B. Schausten, E. Schimpf, K. Eberhardt, M. Eibach, J. Even, D. Hild, J. V. Kratz, L. J. Niewisch, J. Runke, P. Töhrle-Pospiech, N. Wiehl, J. Dvorak, H. Nitsche, J. P. Omtvedt, A. Semchenkov, U. Forsberg, D. Rudolph, J. Uusitalo, L.-L. Andersson, R.-D. Herzberg, E. Parr, Z. Qin, M. Wegrzecki

Pilot-Test Experiment with Os of a SISAK Setup for Hs-Chemistry Studies ***Page 8***
F. Samadani, J. Alstad, F. Schulz, J. Nilssen, J. P. Omtvedt, H. B. Ottesen, S. Qureshi, C. E. Düllmann, J. M. Gates, E. Jäger, J. Khuyagbaatar, J. Krier, M. Schädel, B. Schausten, K. Eberhardt, J. Even, D. Hild, J. V. Kratz, C. Roth, N. Wiehl, A. Türler, A. Yakushev

^{244}Pu-targets for production of element 114 at TASCA ***Page 9***
K. Eberhardt, J. V. Kratz, J. Runke, C. E. Düllmann, B. Lommel, M. Schädel

Recovery of 244Pu from irradiated targets for production of element 114 ***Page 10***
J. Runke, K. Eberhardt, J. V. Kratz, C. E. Düllmann, M. Schädel

Theory

Theoretical Investigations of Trends in Volatility of the Heaviest Elements ***Page 11***
V. Pershina, A. Borschevsky, J. Anton, T. Jacob

Theoretical Investigations of Trends in Adsorption of the Heaviest Elements on Gold ***Page 12***
V. Pershina, A. Borschevsky, J. Anton, T. Jacob

Theoretical Investigations of Chemical Reactivity of Element 113 ***Page 13***
J. Anton, V. Pershina, T. Jacob

Electron Affinity of Element 114, with Comparison to Sn and Pb ***Page 14***
A. Borschevsky, V. Pershina, E. Eliav, U. Kaldor

Production and decay of element 114: high cross sections and new nucleus ^{277}Hs*

Ch.E. Düllmann[1,#], D. Ackermann[1], M. Block[1], W. Brüchle[1], H.G. Essel[1], J.M. Gates[1,2], W. Hartmann[1], F.P. Heßberger[1], A. Hübner[1], E. Jäger[1], J. Khuyagbaatar[1], B. Kindler[1], J. Krier[1], N. Kurz[1], B. Lommel[1], M. Schädel[1], B. Schausten[1], E. Schimpf[1], J. Steiner[1], A. Gorshkov[2], R. Graeger[2], A. Türler[2], A. Yakushev[2], K. Eberhardt[3], J. Even[3], D. Hild[3], J.V. Kratz[3], D. Liebe[3], J. Runke[3], P. Thörle-Pospiech[3], N. Wiehl[3], L.-L. Andersson[4], R.-D. Herzberg[4], E. Parr[4], J. Dvorak[5,6], P.A. Ellison[5,6], K.E. Gregorich[5], H. Nitsche[5,6], S. Lahiri[7], M. Maiti[7], J.P. Omtvedt[8], A. Semchenkov[8], D. Rudolph[9], J. Uusitalo[10], M. Wegrzecki[11]

[1]GSI, Darmstadt, Germany; [2]TU Munich, Garching, Germany; [3]Johannes Gutenberg-University of Mainz, Germany; [4]University of Liverpool, UK; [5]LBNL Berkeley, CA, USA; [6]UC Berkeley, CA, USA; [7]SINP, Kolkata, India; [8]University of Oslo, Norway; [9]Lund University, Sweden; [10]University of Jyväskylä, Finland; [11]ITE, Warsaw, Poland

Introduction

Discoveries of new superheavy elements (SHE) were reported from FLNR, Dubna, Russia [1], including observations of element 114 isotopes produced in ^{48}Ca+^{242,244}Pu reactions. Successful independent studies of some of the reactions studied in Dubna were reported [2,3], most recently also the observation of one atom each of ^{286,287}114 produced in the ^{48}Ca+^{242}Pu reaction at LBNL [4]. Predictions on the existence of an "island of stability" in the region of SHE have substantiated, despite the small number of observed events in every confirmation experiment. All successful confirmation experiments reported cross sections lower than those from FLNR by factors of two or more. Nevertheless, these cross sections are unexpectedly high compared to extrapolations from lighter systems [5], and intriguingly constant over a large range of $112 \le Z \le 118$. A thorough understanding of the underlying production mechanism is still missing; location and extension of the "island of stability" in the region of spherical SHE is still far from being established. To help shedding more light on these problems, a ^{48}Ca+^{244}Pu experiment was performed at the gas-filled TransActinide Separator and Chemistry Apparatus (TASCA) [6,7], which was optimized for the study of ^{48}Ca-induced fusion reactions with actinide targets. TASCA's efficiency for this nuclear reaction type is currently unsurpassed.

Experimental

The UNILAC accelerated a pulsed ^{48}Ca beam (~$2 \cdot 10^{12}$ s^{-1}), which passed through $^{244}PuO_2$ targets (average thickness: 438 μg/cm^2 ^{244}Pu). Beam energies inside the targets were 241.3-246.2 MeV (E*=39.8-43.9 MeV; hereafter referred to as 42-MeV run) and 236.4-241.0 MeV (E*=36.1-39.5 MeV; 38-MeV run). $2.44 \cdot 10^{18}$ (42-MeV run) and $1.15 \cdot 10^{18}$ (38-MeV run) projectiles passed through the targets. Nuclear reaction products entered TASCA, operated in "high transmission mode" [7], and were separated in 0.8 mbar He gas. The detection system consisted of a Multi Wire Proportional Counter (MWPC) and a focal plane detector box (FPDB). The FPDB consisted of a Double Sided Silicon Strip Detector (DSSSD; pitch size: 1 mm; 144 vertical / 48 horizontal strips) and Single Sided Silicon Strip Detectors (SSSSD) mounted perpendicular in the backward hemisphere of the DSSSD [8]. The MWPC provided a signal for ions recoiling from the target and allowed distinguishing these from radioactive decays of species implanted in the DSSSD. The energy resolution of the FPDB was 25 keV FWHM for 8.1 MeV α-particles fully stopped in the DSSSD and 170 keV for α-particles that deposited a fraction of their energy inside the DSSSD and the remainder in the SSSSD. The detection efficiency was 72% for α-particles and 100% for SF. The efficiency for focusing element 114 EVRs into the DSSSD was (60±6)% [9]. Data acquisition was triggered by events registering more than 300 keV in the DSSSD or more than 500 keV in a SSSSD. More details are given in [10,11].

Results

We searched [12] for decay chains from ^{288,289}114 exhibiting the decay patterns as published in [1]. Afterwards, upon identification of a chain, additional α-particles occurring in the same pixel as the chain were searched for, in between registration of the EVR and the terminating SF. Based on the event rate only 0.02 (^{289}114) and 0.05 (^{288}114) random chains from unrelated background events were expected. The search yielded nine EVR-α-SF chains (^{288}114) and four EVR-α-α(-α)-SF chains (^{289}114). Ten chains were measured in the 42-MeV run and three chains in the 38-MeV run (Figs. 1 and 2). The agreement of our data (Table 1) with that of [1] is good in all cases except for chain #9. The data measured for the EVR, the first, and the second α-particle suggest assigning chain #9 to $^{289}114 \rightarrow ^{285}112 \rightarrow ^{281}$Ds. ^{281}Ds then decayed by emission of a (8.727±0.025)-MeV α-particle 5.688 s after the decay of ^{285}112, during the beam-off period, where background is low. ^{281}Ds has undergone SF in all ten previously observed decays [1] with $T_{1/2} = 11.1^{+5.0}_{-2.7}$ s. Based on background rates, the probability to register

* Work supported by the BMBF (06MT247I, 06MT248, 06MZ223I); the GSI-F&E (MT/TÜR, MZJVKR); the Swedish and Norwegian (177538) Science Councils; the US DOE (DE-AC03-76SF00098; DE-AC02-05CH11231; NNSA Fellowship); the Govt. of India (TADDS).

#c.e.duellmann@gsi.de

an α-like event with properties as exhibited by the observed one is only 0.1%. We thus assign it to a so far unobserved α-branch in ^{281}Ds. Considering this α-decay and the thirteen measured SF decays from [1] and our work, an α-decay branch b_α of 9^{+16}_{-7} % results after correcting for detection efficiency differences for α-decay and SF. The chain was terminated 4.5 ms later by SF of the new nucleus ^{277}Hs.

The B•ρ of element 114 EVRs in 0.8 mbar He was measured to (2.29±0.11) T•m.

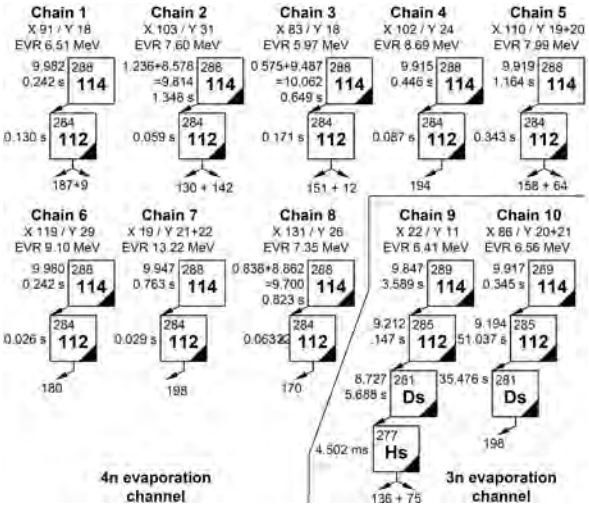

Figure 1: Decay chains assigned to ^{288}114 (chains 1-8) and ^{289}114 (chains 9, 10) observed during the 42-MeV run. A black triangle in the lower right corner of a box indicates that the beam was off at the time of the event.

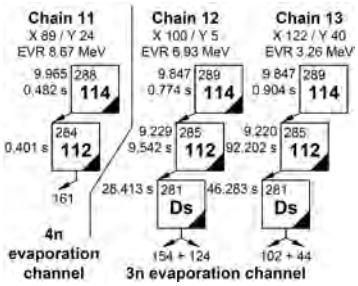

Figure 2: Same as Figure 1, but showing decay chains observed during the 38-MeV run.

Table 1. Decay properties (this work combined with [1])

Isotope	Decay	$T_{1/2}$ (this work)	$T_{1/2}$ (combined)
^{289}114	α	$0.97^{+0.97}_{-0.32}$ s	$2.1^{+0.8}_{-0.4}$ s
^{288}114	α	$0.47^{+0.24}_{-0.12}$ s	$0.69^{+0.17}_{-0.11}$ s
^{285}112	α	30^{+30}_{-10} s	29^{+11}_{-6} s
^{284}112	SF	101^{+50}_{-25} ms	99^{+24}_{-16} ms
^{281}Ds	SF/α:91/9	20^{+20}_{-7} s	13^{+5}_{-3} s
^{277}Hs	SF	3^{+15}_{-1} ms	3^{+15}_{-1} ms

Discussion

Z=108 is a deformed proton shell closure in N~162 isotopes. The observed ^{277}Hs lifetime is short compared to half-lives of the Hs isotopes near the deformed N=162 shell closure, indicating reduced shell stabilization in the N=169 nucleus ^{277}Hs. Macro-microscopic model predictions of $T_{1/2}$(SF) for the neighboring isotopes are 46 ms (^{276}Hs) and 0.98 ms (^{278}Hs), the geometric mean being 6.7 ms [13]. This is similar to our observed lifetime. The odd neutron is expected to hinder SF decay significantly. Thus, the drop in $T_{1/2}$(SF) when increasing N above 162 may be more severe than suggested by [13]. ^{275}Hs (N=167) decays by α-particle emission with $T_{1/2}$=0.19 s [1]. The experimental trend with prevalent α-decay in Hs isotopes with N=157-167, but predominant SF in lighter as well as in heavier isotopes is close to that in [10], which suggests dominant α-decay from N=154 to N=166 but SF for N>168. This indicates that stability vanishes rapidly with increasing distance from N=162.

Measured cross sections for element 114 isotopes in the 38-MeV run were $8.0^{+7.4}_{-4.5}$ pb (3n channel) and $2.8^{+4.2}_{-2.1}$ pb (4n channel), and in the 42-MeV run, $3.5^{+3.3}_{-2.0}$ pb (3n channel) and $9.8^{+3.9}_{-3.1}$ pb (4n channel). Error bars include statistical uncertainties only (68.3% confidence level); the systematic uncertainty is estimated to 14%. In contrast to any other confirmation experiment, we confirm the large cross sections as reported from FLNR [1]. In fact, our measured cross sections are higher than those reported from the DGFRS. These high cross sections call for investigations of the details of the production mechanism. Production rates that follow from these values encourage using this nuclear reaction to produce relatively long-lived isotopes of element 114, in particular for envisaged chemical investigations [14] or for γ-spectroscopic studies that allow shedding light on the nuclear structure in this SHE region and may facilitate unique Z identification.

We thank the ECR and UNILAC staff for excellent ^{48}Ca beams and H. Brand and the GSI EE department, the machine shop staff at the institute of radiochemistry, TU Munich, and V. Gorshkov for technical support.

References

[1] Yu.Ts. Oganessian, J. Phys. G 34 (2007) R165.
[2] S. Hofmann, EPJA 32 (2007) 251.
[3] R. Eichler et al. Nature 447 (2007) 72.
[4] L. Stavsetra et al., PRL 103 (2009) 132502.
[5] S. Hofmann, Lect. Notes Phys. 264 (2009) 203.
[6] M. Schädel, Eur. Phys. J. D 45 (2007) 67.
[7] A. Semchenkov et al., NIM B 266 (2008) 4153
[8] A. Gorshkov et al., in preparation for NIM A.
[9] K.E. Gregorich et al., GSI Sci. Rep. 2006 (2007) 144.
[10] Ch.E. Düllmann et al., submitted to PRL.
[11] J.M. Gates et al., in preparation for PRC.
[12] H.G. Essel et al., this Scientific Report.
[13] R. Smolanczuk, PRC 52 (1995) 1871.
[14] A. Yakushev et al., this Scientific Report.

The Performance of TASCA in the ^{48}Ca+^{206,207,208}Pb Reactions

J. Khuyagbaatar[1], M. Schädel[1], D. Ackermann[1], Ch.E. Düllmann[1], E. Jäger[1], F.P. Heßberger[1], A. Semchenkov[1,2], A. Gorshkov[2], R. Graeger[2], A. Türler[2], A. Yakushev[2], K. Eberhardt[3], J. Even[3], J.V. Kratz[3], L.-L. Andersson[4], D. Rudolph[4] for the TASCA Collaboration

[1]GSI, Darmstadt, Germany; [2]Technical University München, Garching, Germany; [3]University of Mainz, Mainz, Germany; [4]Lund University, Lund, Sweden

The gas-filled recoil separator TASCA (**T**rans**A**ctinide **S**eparator and **C**hemistry **A**pparatus) was installed in a dipole-quadrupole-quadrupole configuration (DQQ) at the UNILAC at GSI [1-3]. An extensive commissioning program [4] was carried out at TASCA studying a large number of experimental parameters and nuclear reactions. Depending on the polarity of the quadrupole magnets TASCA can be operated in two modes: the so called High Transmission Mode (HTM) and the Small Image Mode (SIM). Dispersion values of 9 and 1 mm per one percent change of $B\rho$ were calculated for the HTM and SIM, respectively [3]. Ion optical calculations of the HTM and SIM were performed using Monte-Carlo simulations [5].
Important characteristics of TASCA in both modes were investigated using ^{48}Ca+Pb reactions and a 16-strip 80x35 mm^2 large position-sensitive silicon-strip detector based focal plane detector (FPD). Optimal magnetic settings and gas pressures were established by centering spatial distributions of α-decaying evaporation residues in the FPD. Transmission measurements were performed with targets of well determined thicknesses.

HTM:

Measured spatial distributions of ^{254}No ions are shown in Fig. 1 for different helium gas pressures and a constant dipole magnet setting of $B\rho$=2.08 Tm. Solid curves show the calculated [5] distribution of ^{254}No ions in the FPD of TASCA at different gas pressures. Well centered distributions were observed in the range of 0.8 to 1.0 mbar pressure range. These distributions are in very good agreement with the calculated ones. However, at lower and higher gas pressures the ^{254}No distributions are horizontally shifted off-center. This means that the deflection angle of ^{254}No in the dipole magnet is changing. This is related to a change of average charge of ^{254}No ions. Such an effect was observed also at the Dubna gas-filled separator and it was explained with so-called "density effect" [6].
An average value of (57±5) % for the transmission of No isotopes synthesized in ^{48}Ca on $^{206-208}$Pb reactions was deduced using the cross-section data for fusion-evaporation reactions from [7]. This value is in good agreement with the calculated value of about 52 % for the HTM of TASCA.

SIM:

To find optimal settings for the quadrupole magnets in the SIM is more difficult than for the HTM. Various settings for the quadrupole focusing were tested to obtain best values. A 40-mm diameter image size was taken as a "reference" best value. Again, deviations between this optimized result, which is in agreement with theoretical calculations, and distributions obtained at pressures lower than the optimal He pressures were observed.
A transmission of (35±5) % was deduced at optimized SIM settings for the reaction ^{48}Ca+^{208}Pb. This value is in good agreement with calculated values.

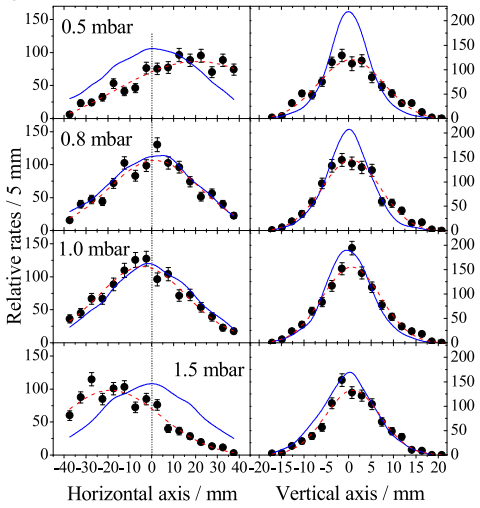

Fig 1: Spatial distributions of ^{254}No ions in the FPD at different pressures of the He filling-gas. TASCA was operated in HTM. Dashed lines show the Gaussian fit.

Pure hydrogen and He-H_2-mixtures were used as filling gases in both modes as well. The optimal magnetic settings and gas pressures were investigated and the corresponding average charges of nobelium ions were determined. Within a 10% uncertainty, the measured transmissions for He, H_2 and mixtures of both gases were identical. When pure H_2 and a mixture of He and H_2 were used, we observed a better background suppression of target-like ions as compared with pure helium.
More detailed information on the TASCA performance in ^{48}Ca+Pb reactions and average charges of the nobelium ions in various gases will be given in [8].

[1] M. Schädel, Eur. Phys. J. D 45 (2007) 67. See also www.gsi.de/TASCA.
[2] M. Schädel, J. Nucl. Radiochem. Sci. 8 (2007) 47.
[3] A. Semchenkov et al., NIM B 266 (2008) 4153.
[4] M. Schädel et al., GSI Sci. Rep. 2008 (2009) 138.
[5] K.E. Gregorich et al., GSI Sci. Rep. 2006 (2007) 144.
[6] Yu.Ts. Oganessian et al., PRC 64 (2001) 064309.
[7] Yu.Ts. Oganessian et al., PRC 64 (2001) 054606.
[8] J. Khuyagbaatar et al., to be published.

TASISpec – Heading towards its first experiment.

L.-L. Andersson[1], D. Rudolph[2], D. Ackermann[3], Ch.E. Düllmann[3], K. Eberhardt[4], J. Even[4], U. Forsberg[2], J. Gellanki[2], J. Gerl[3], P. Golubev[2], R. Hoischen[2,3], R.-D. Herzberg[1], F.P. Heßberger[3], E. Jäger[3], J. Khuyagbaatar[3], I. Kojouharov[3], J.V. Kratz[4], J. Krier[3], N. Kurz[3], E. Merchán[3], W. Prokopowicz[3], M. Schädel[3], H. Schaffner[3], B. Schausten[3], E. Schimpf[3], A. Semchenkov[5,6], A. Türler[5,7], H.-J. Wollersheim[3], A. Yakushev[5], and P. Thörle-Pospiech[4]

[1]University of Liverpool, Oliver Lodge Laboratory, Liverpool L69 7ZE, United Kingdom; [2]Department of Physics, Lund University, S-22100 Lund, Sweden; [3]GSI Helmholtzzentrum für Schwerionenforschung GmbH, D-64291 Darmstadt, Germany; [4]Universität Mainz, D-55128 Mainz, Germany; [5]Technische Universität München, D-85748 Garching, Germany; [6]University of Oslo, 0315 Oslo, Norway; [7]Paul Scherrer Institute, 5232 Villigen, Switzerland

TASISpec (*TA*sca *S*mall *I*mage mode *Spec*troscopy) [1, 2] is a Si and Ge detector setup optimised for particle-γ-X-ray coincidence spectroscopy of superheavy elements in conjunction with the TASCA separator [3]. The detection system consists of 192 Si strips distributed over one double sided silicon strip detector (DSSSD) and four single sided silicon strip detectors (SSSSD). The DSSSD is the focal plane detector into which the residual nuclei are implanted and their subsequent decay products such as fission fragments or α particles are detected. The SSSSDs form a "box" upstream from the DSSSD and they are used to detect α particles which have escaped detection in the DSSSD, conversion electrons (CE) and possibly the second fission fragment. A seven-crystal Ge cluster detector is mounted directly behind the DSSSD and four clover detectors are mounted behind the four SSSSDs. The complete setup is thus composed of a total of 23 Ge crystals.

The setup is constructed to enable multi-coincidence spectroscopy such as α-γ-CE and α-γ-γ with unprecedented γ-ray efficiency and thus reveal essential information necessary to build reliable level schemes for superheavy elements.

During 2009 a thorough evaluation of the commissioning experiments was performed [2]. This involved amongst others detection efficiencies and implant-decay correlation times. As an example, the decay of ^{253}No has been explored. The half life of the ground state was previously determined to $T_{1/2} = 1.56(2)$ min [4]. In the present analysis the half life is determined to $T_{1/2} = 1.61(21)$ min where the uncertainty originates mainly from the small number of α particles, which could be included in the analysis. In Fig. 1 the DSSSD hitpattern is shown. It shows the pixels in which the 8.0 MeV α particles relating to the decay of the ground state of ^{253}No were detected. As can be seen in this figure the implants are nicely focused into a very narrow spot. Since the half life of ^{253}No is rather long the pixels in the very centre of the focal spot where the implantation rates are at its highest, were excluded when determining the half life. This minimises the risk of random correlations between the incoming evaporation residues and the α particles.

In a commissioning run in July 2009 was the reaction ^{208}Pb(^{48}Ca,$1n$)^{255}No applied to explore the benefits gained from the usage of pulse-shape electronics. Pulse shape analysis could yield particle identification due to distinct ionisation schemes in the semiconductor material for different incidenting particles, like e.g. α particles and CE.

In the beginning of 2009 TASISpec was granted beamtime for its first main beam experiment. The experiment is scheduled for spring 2010 and will aim to explore K-isomers in ^{253}No in detail.

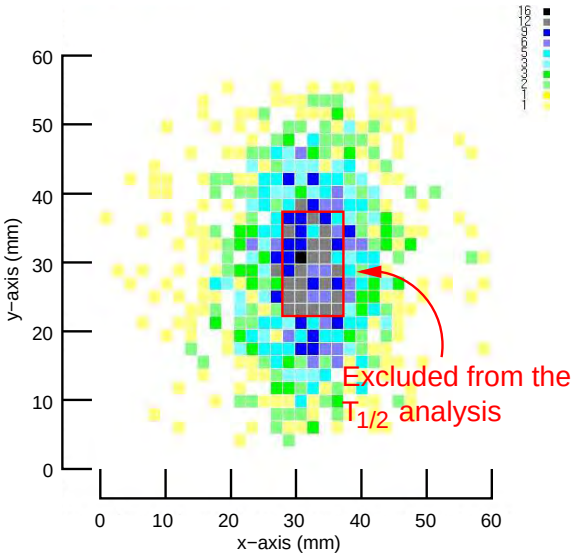

Figure 1: The position of the detected ^{253}No correlated alpha particles in the DSSSD. On the x and y-axis the size of the DSSSD is indicated.

References

[1] L. -L. Andersson *et al.* GSI Scientific report 2008. `http://www-wnt.gsi.de/kernchemie/images/PDF_2008/NUSTAR-SHE-11.pdf`

[2] L. -L. Andersson *et al.*, submitted to Nucl. Instrum. Meth.

[3] A. Semchenkov *et al.*, Nucl. Instrum. Meth. Phys. Res. B **266**, 4153 (2008).

[4] R.-D. Herzberg *et al.*, Eur. Phys. J. A (2009).

A new TASCA focal plane detector setup and DAQ system*

A. Gorshkov[1#], J.M. Gates[1,2], R. Graeger[1], A. Türler[1†], A. Yakushev[1], D. Ackermann[2], W. Brüchle[2], Ch.E. Düllmann[2], H.G. Essel[2], E. Jäger[2], J. Khuyagbaatar[2], I. Kojouharov[2], J. Krier[2], N. Kurz[2], M. Schädel[2], B. Schausten[2], E. Schimpf[2], J. Dvorak[3,4], L.-L. Andersson[5], D. Rudolph[6], M. Wegrzecki[7]

[1]TU Munich, Garching, Germany; [2]GSI, Darmstadt, Germany; [3]LBNL, Berkeley, CA, U.S.A; [4]University of California, Berkeley, CA, U.S.A.; [5]University of Liverpool, UK; [6]University of Lund, Sweden; [7]ITE, Warsaw, Poland

During the TASCA commissioning phase competitive tests of two types of focal plane detectors for TASCA – a Position Sensitive Silicon Stripe Detector (PSSSD) and a Double Sided Silicon Strip Detector (DSSSD) - have been performed. The DSSSD proved to be more reliable and more sensitive for the detection of decay chains due to the high granularity of the DSSSD; moreover the position resolution of the DSSSD is independent of implantation position and deposited energy [1, 2]. The new TASCA focal plane detector setup consists of a Multi Wire Proportional Counter (MWPC) and a Focal Plane Detector Box (FPDB). The implantation detector of the FPDB consists of two side-by-side mounted 300 μm-thick DSSSDs with an active size of 72x48 mm^2 each mounted on a PCB frame. Eight 500 μm-thick Single Sided Silicon Strip Detectors (SSSSD) of the same size form a backward array – a four-sided box with an open side of 144x48 mm^2 and a depth of 72 mm (Fig. 1) [3]. The DSSSD comprises 144 vertical strips on the front side and 48 horizontal strips on the back side, each with 1 mm pitch size. Spectrometric signals are read out from the front and back sides. They provide implantation and decay energies and (x,y) coordinates with a position resolution of 1 mm. While the registration efficiency from the back side is almost 100%, the one from the front side is about 90% due to a gap of 100 μm between the strips. Each SSSSD has 8 strips with an active area 5.7x72 mm^2 without position resolution. The energy resolution in the DSSSD was ≤25 keV (FWHM) for 8.1 MeV α-particles measured with implanted ^{254}No depositing their full energy in the DSSSD and 170 keV for reconstructed α-particles that deposited a fraction of their energy inside the DSSSD and the remainder in the SSSSD. The average detection efficiency of the FPDB for α-particles emitted from a nucleus implanted in the active area of the DSSSD is 72%. Two additional SSSSDs are mounted behind the implantation detector and serve as a punch-through veto detector for light fast ions. The punch-through detector together with the MWPC serves for discriminating between ions recoiling from the target, radioactive decays of implanted species, and fast light ions. A cluster Ge-detector consisting of seven crystals was installed ~30 mm behind the FPDB for γ-ray measurements in coincidence with α- or SF decays.

In total 640 spectrometric channels (320 for the α-particle branch and 320 for the SF branch) are required to readout the FPDB. To minimize the total number of ADC channels, 8-channel dual-range amplifiers with integrated multiplexers were built. 40 analog output signals from the α-particle branch and 40 ones from the SF branch are connected to inputs of three V785 32-channel peak sensing ADCs (CAEN). 40 digital 3-bit outputs from the amplifiers with address codes of the fired strips are stored in four SIS 3820-3600 32-channel I/O VME registers (Struck GmbH). Analog signals from Ge-detectors are digitized in the SIS 3302 8-channel 100 MS/s 16-bit flash ADC (Struck GmbH). The amplifiers have a logical trigger output with adjustable discriminator level. All trigger outputs from the amplifiers are collected by "OR" in a CAMAC Common Trigger module. When a processed common trigger signal is accepted by a VME trigger module TRIVA5, the amplitudes of all fired ADC channels, the status of all registers, and time stamps are read out by a RIO4 (CES) frontend VME controller using the MBS software package. The total readout dead time was about 50 μs; a shorter dead time of ~30 μs was measured without Ge-detectors reading. Visualization as well as on-line and off-line analysis was performed using the software package GO4 [4].

The new detector setup and new DAQ system have been successfully used during the experiment on the synthesis of element 114 performed at TASCA in 2009 [5].

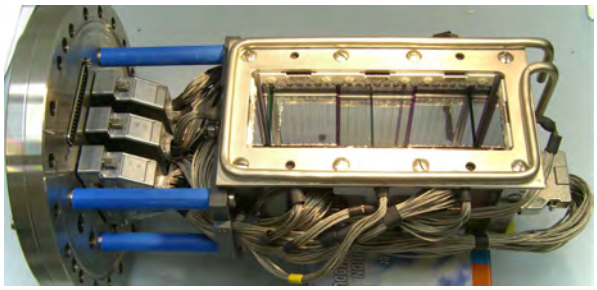

Figure 1: The new DSSSD-based TASCA FPDB.

References

[1] A. Gorshkov et al., GSI Sci. Rep. 2008, p. 140,
[2] A. Gorshkov et al., Phys. Rev. C, to be submitted.
[3] A. Gorskov et al., NIM A, to be submitted.
[4] H.G. Essel et al., GSI Sci. Report 2009, p. ???
[5] Ch.E. Düllmann et al., GSI Sci. Report 2009, p. ???

* Work supported by the BMBF (06MT247I, 06MT248); the GSI-F&E (MT/TÜR).

†Current address: Bern University & PSI Villigen, Switzerland
#alexander.gorshkov@radiochemie.de

COMPACT Coupled to TASCA for Element 114 Chemistry*

A. Yakushev[1#], J.M. Gates[1,2], A. Gorshkov[1], R. Graeger[1], A. Türler[1†], D. Ackermann[2], M. Block[2], W. Brüchle[2], Ch.E. Düllmann[2,3], H.G. Essel[2], F.P. Heßberger[2,3], A. Hübner[2], E. Jäger[2], J. Khuyagbaatar[2], B. Kindler[2], J. Krier[2], N. Kurz[2], B. Lommel[2], M. Schädel[2], B. Schausten[2], E. Schimpf[2], K. Eberhardt[4], M. Eibach[4], J. Even[4], D. Hild[4], J.V. Kratz[4], L.J. Niewisch[4], J. Runke[4], P. Töhrle-Pospiech[4], N. Wiehl[4], J. Dvorak[5,6], H. Nitsche[5,6], J.P Omtvedt[7], A. Semchenkov[7], U. Forsberg[8], D. Rudolph[8], J. Uusitalo[9], L.-L. Andersson[10], R.-D. Herzberg[10], E. Parr[10], Z. Qin[11], M. Wegrzecki[12]

[1]TU Munich, Garching, Germany; [2]GSI, Darmstadt, Germany; [3]Helmholtz Institute Mainz, Germany; [4]University of Mainz, Germany; [5]LBNL, Berkeley, CA, U.S.A; [6]University of California, Berkeley, CA, U.S.A.; [7]University of Oslo, Norway; [8]Lund University, Sweden; [9]University of Jyväskylä, Finland; [10]University of Liverpool, UK; [11]IMP, Lanzhou, P.R. China, [12]ITE, Warsaw, Poland

The unambiguous identification of new superheavy elements (SHE) is a very difficult task for both, physicists and chemists due to very low production rates, absence of a link to known isotopes, and unknown chemical, and decay properties. Chemical studies of SHE are of great importance because they can identify the proton number of the studied isotopes. Coupling of chemistry setups to physical recoil separators allows chemical experiments with extremely high sensitivity due to a strong suppression of unwanted byproducts in the preseparator [1]. At GSI, the new gas-filled separator TASCA has been put into operation in 2008. It is designed specifically for chemical studies of transactinides produced in nuclear fusion reactions of ^{48}Ca beams with actinide targets [2].

The highest cross section for SHE formation was observed in the reaction ^{48}Ca+^{244}Pu [3,4] leading to element 114 (E114). First attempts to chemically identify E114 were performed by a PSI-FLNR-LLNL collaboration in Dubna, and an unexpectedly low adsorption enthalpy of element 114 on gold was reported [5], in contradiction with theoretical predictions of the trend in the binding energy, E_b, Pb>>E114>Hg>E112 [6]. These studies were performed without preseparation, and the relatively high counting rate from unwanted byproducts led to controversially discussed results. An attempt to observe E114 in the chemistry experiment after preseparation failed [7].

A chemistry experiment with E114 was carried out at TASCA in 2009. Because the lifetimes of even the longest-lived E114 isotopes, ^{288,289}114, are short [4], TASCA was operated in the Small Image Mode (SIM) [2], which focuses fusion products into a small area of about ~30x40 mm^2. The lower transmission efficiency of SIM (~35%) compared to HTM (~60%) is compensated by the smaller volume of the Recoil Transfer Chamber (RTC), which allows a faster transport of products to a detection setup. During the experiment on the synthesis of ^{288,289}114 [4], the operation of TASCA in SIM was successfully tested with a focal plane detector. A beam dose of $0.98 \cdot 10^{18}$ ^{48}Ca ions at E*(^{292}114)=42 MeV was acquired and two ^{288}114 decay chains were observed. In the preparation of the experiment two RTCs made of Teflon™ were tested: a "small" one with a volume of 14 cm^3 and a "large" one with 29 cm^3. Transport times and yields to COMPACT [8] were optimized for both chambers with short-lived Hg and Pb isotopes produced with ^{40}Ar and ^{48}Ca beams. Transport times of 0.6 s and 0.8 s were measured at a gas flow rate 1.3 l/min for the "small" and "large" RTC, respectively. Three different He/Ar gas mixtures with ratios of 30:70, 50:50, and 70:30 were explored. The last one was selected for the E114 chemistry experiment. Two similar COMPACT detectors connected in series were used; each detector consisted of 32 pairs of 1x1 cm^2 PIN diodes covered with a 35-nm thick gold layer. The first detector, kept at the room temperature, was connected directly to the RTC exit via a 2-cm long Teflon™ tube. The second detector, connected via a 30-cm long Teflon™ capillary, was placed downstream of the first one; a temperature gradient from +20 to −162 °C was applied along it. The use of two detectors in series allows detecting species in a wide range of volatilities – from the non-volatile Pb to the noble gas Rn (Fig. 1). With this setup the adsorption enthalpy of short-lived ^{288,289}114 on gold was measured with relatively high efficiency under background-free conditions. The data are under evaluation.

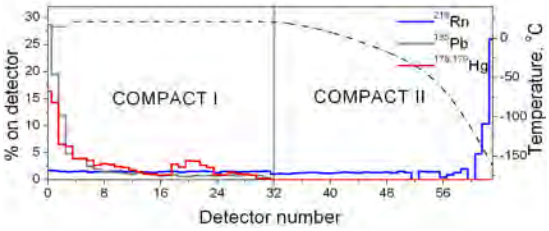

Figure1:Pb, Hg and Rn distributions in COMPACT.

References

[1] Ch. E. Düllmann, Eur. Phys. J. D **45**, 75 (2007).
[2] A. Semchenkov et al. NIM B **266**, 4153 (2008).
[3] Yu. Oganessian, J. Phys. G **34**, R165 (2007).
[4] Ch. E. Düllmann et al. This report, p.???(2010).
[5] R. Eichler et al. Radiochim. Acta, accepted (2009).
[6] V. Pershina et al. J. Chem. Phys. **131**, 084713 (2009).
[7] D. Wittwer et al. Nucl. Instr. Meth. B **268,** 28 (2010).
[8] J. Dvorak et al. Phys. Rev. Lett. **97,** 242501 (2006).

* Work supported by the BMBF (06MT247I, 06MT248); the GSI-F&E (MT/TÜR).

†Current address: Bern University & PSI Villigen, Switzerland
#alexander.yakushev@radiochemie.de

Pilot-Test Experiment with Os of a SISAK Setup for Hs-Chemistry Studies

F. Samadani[1], J. Alstad[1], F. Schulz[1], J. Nilssen[1], J.P. Omtvedt[1], H.B. Ottesen[1], S. Qureshi[1], Ch.E. Düllmann[2], J.M. Gates[2], E. Jäger[2], J. Khuyagbaatar[2], J. Krier[2],M. Schädel[2], B. Schausten[2], K. Eberhardt[3], J. Even[3], D. Hild[3], J.V. Kratz[3], Ch. Roth[3], N. Wiehl[3], A. Türler[4], A. Yakushev[4]

[1]University of Oslo, Norway, [2]GSI, Darmstadt, Germany, [3]Johannes Gutenberg-University of Mainz, Germany, [4]TU Munich, Garching, Germany

A liquid-liquid extraction system for investigating chemical properties of element 108, hassium, was developed [1] using γ-emitting ^{181}Os produced at the Oslo Cyclotron Laboratory (OCL). The system is targeted for the fast solvent extraction system SISAK [2] and based on OsO_4 reacting with NaOH. Such an experiment would be the first attempt to study Hs in the liquid phase. Successful Rf and Db experiments [3-5] performed at LBNL in Berkeley indicate that SISAK with its liquid scintillation detectors is sensitive enough to detect Hs, even though the Hs cross section is ~3 orders of magnitude lower.

The first investigation of the reaction between HsO_4 and NaOH was performed in a gas phase experiment [6]. The interaction of HsO_4 appeared somewhat weaker with NaOH than that of OsO_4, in fair agreement with theoretical predictions [7]. The liquid-liquid extraction Hs-experiment proposed in the work presented here is based on results from this gas-phase experiment. In aqueous solution, it is assumed [1] that the reactions occurring are:

$$OsO_4(aq) + NaOH(aq) \leftrightarrow Na[OsO_4(OH)](aq) \quad (1)$$

$$Na[OsO_4(OH)] + NaOH \leftrightarrow Na_2[OsO_4(OH)_2] \quad (2)$$

$$OsO_4(aq) \rightarrow OsO_4(org) \quad (3)$$

The distribution ratio between NaOH solution and toluene, which was selected as organic phase because it is also suitable as solvent for the liquid scintillation detection used by SISAK, is given by:

$$D = \frac{[OsO_4]_{org}}{[OsO_4]_{aq} + [OsO_4(OH)]^- + [OsO_4(OH)_2]^{2-}} \quad (4)$$

which can be rewritten as:

$$D = \frac{K_D}{1 + K_1[OH^-] + K_1K_2[OH^-]^2} \quad (5)$$

where K_1, K_2 and K_D are equilibrium constants for reactions (1), (2), and (3), respectively. Experiments were performed in Oslo, utilizing manual extractions and SISAK on-line measurements to carefully study the behavior of Os in this chemical system, see Samadani et al. [1] for details. The results are summarized in Fig. 1.

Based on the results from Oslo a "proof-of-principle" experiment with α-decaying Os isotopes was performed at GSI: the full SISAK setup [8], as it would be used for a Hs experiment with double α-detector arrays to simultaneously measure both phases (for the aqueous phase done indirectly, after a second extraction step) was set up and tested. $^{40}Ar^{11+}$ ions from the UNILAC irradiated a ^{nat}Ce target in the gas-filled separator TASCA (TransActinide Separator and Chemistry Apparatus) producing $^{172-175}$Os.

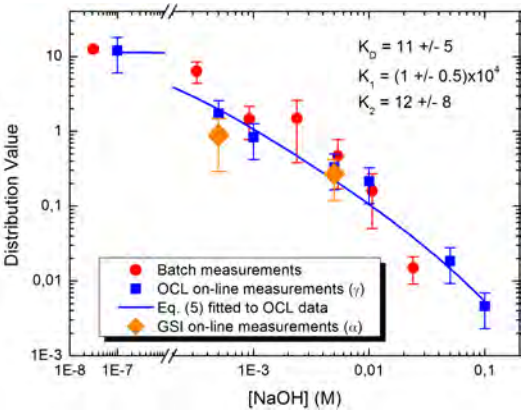

Figure 1: Comparison of data from OCL and GSI, together with fit of eq. (5) to OCL data.

In the separator focal plane a Recoil Transfer Chamber (RTC) was mounted. It was flushed with a He/O_2 gas mixture, which passed an oven (run at 600°C) mounted at the exit of the RTC to ensure fast and complete oxidation of Os. The volatile osmium tetroxide was transported to SISAK by the He/O_2 gas and dissolved in NaOH solution. After extraction into toluene the α-activity was measured in on-line flow cells by liquid scintillation detection. This was the first SISAK experiment behind TASCA. Results from this run using α-decaying ^{172}Os agree well with those of γ-measurements obtained in Oslo, as shown in Fig. 1. This successful experiment proved that the system is suitable for studying Hs.

References

[1] F. Samadani et al., "Development of a SISAK extraction system for chemical studies of element 108, hassium", submitted to Radiochim. Acta.

[2] J.P. Omtvedt et al., J. Alloy Comp. **271-273**, 303 (1998).

[3] J.P. Omtvedt et al., Journ. Nucl. Radiochem. Sciences, **3**, 121 (2002).

[4] L. Stavsetra et al., Nucl. Instrum. Method Phys. Res. Sect. A, **543**, 509 (2005).

[5] J.P. Omtvedt et al. "Detection of ^{258}Db with the SISAK Liquid Scintillation Detection System", manuscript in preparation for Radiochim. Acta.

[6] A. von Zweidorf et al., Radiochim. Acta, **92**, 855 (2004).

[7] V. Pershina, Radiochim. Acta, **93**, 373-376 (2005).

[8] J.P Omtvedt, et al., Eur. Phys. J. D, **45**, 91 (2007).

^{244}Pu-targets for production of element 114 at TASCA*

K. Eberhardt[1,#], J. V. Kratz[1], J. Runke[1], Ch. E. Düllmann[2], B. Lommel[2] and M. Schädel[2]
[1]Institut für Kernchemie, Johannes Gutenberg-Universität Mainz, Germany; [2]GSI, Darmstadt, Germany

Introduction

In a series of recent experiments at TASCA, production and decay as well as chemical properties of element 114 have been investigated using the ^{244}Pu(^{48}Ca,3/4n)-reaction leading to ^{288,289}114 [1,2]. Because the ^{244}Pu target material is available only in very limited amounts, the target preparation technique should give high yields. Easy and complete recovery of the target material is another prerequisite [3]. Thus, we have chosen Molecular Plating (MP) onto 2 µm thin pinhole-free titanium foils as the target preparation technique. At TASCA, a rotating target wheel is used composed of three banana-shaped target segments with an active target area of 1.44 cm^2 each. The rotating target is confined in a nearly closed container in order to protect the beam line as well as the separator against contamination in the case that a target gets destroyed.

^{244}Pu target production and characterization

For the production of one target segment by MP about 1 mg of ^{244}Pu in the form of its nitrate is dissolved in a small volume (100-200 µl) of nitric acid in a Teflon™ beaker and mixed with a surplus of isopropanol (800 µl). The mixture is then transferred into the electrochemical deposition cell (EDC) made of Teflon™ which is subsequently filled up with isobutanol to a total volume of 16 ml [4]. MP is carried out by applying a voltage of 150-200 V at a maximum current density of about 1.2 mA/cm^2. After 5-6 hours plating time, deposition yields up to 90 % are achieved. The backing foils are produced by cold rolling at GSI [5]. They should be pinhole-free and are pre-cleaned with isopropanol, 6 M hydrochloric acid and water. Prior to use, the foil integrity is checked by optical microscopy to ensure that the backing is pinhole-free. The average foil thickness is determined by weighing, whereas the homogeneity of the foil thickness is checked by α-particle energy-loss measurements. For a target backing foil with a nominal thickness of 2.2 µm deviations are in the order of ± 0.2 µm.

The target thickness is determined by two independent methods: (i) *α-particle spectroscopy*. After the deposition is completed, the target is dismounted from the EDC, dried under an infrared lamp and measured with a surface barrier α-detector at a distance of about 30 cm. (ii) The Pu-content of the solution in the EDC is determined by *Neutron Activation Analysis*. Subsequent to MP an aliquot of the supernatant solution in the EDC (1 ml) is irradiated for 2 h in the TRIGA Mainz research reactor with a thermal neutron flux of 7 x 10^{11} cm^{-2}s^{-1}. Here, 10.5 h-^{245}Pu is formed via the reaction ^{244}Pu(n,γ)^{245}Pu.

*Supported by the GSI F&E (MZJVKR).
#klaus.eberhardt@uni-mainz.de

The Pu content of the irradiated solution is determined by means of γ-spectrometry using the prominent γ-lines resulting from the ^{245}Pu decay at 327 keV, 308 keV, and 560 keV, respectively [3]. Table 1 comprises all ^{244}Pu-targets produced for TASCA so far.

Table 1: ^{244}Pu-targets for TASCA

Target#	Thickness [µg/cm^2]
08-395	401
08-482	502
08-485	490
08-486	390
08-487	472
09-562	673
09-594	724
09-623	790
09-624	785

The homogeneity of the Pu-layer is checked with radiography [6] using a commercial radiographic imager (FLA 7000 from FUJIFILM Corp.). Figure 1 shows a picture of a target segment. Here, the brown layer indicates the Pu-oxide deposit. Also shown is a 3-dimensional plot of the activity distribution. With this technique it could be shown that the active target area is completely covered and, in addition, that Pu is homogeneously distributed over the entire target area. From this one can conclude that variations in target thickness are in the order of about 15%.

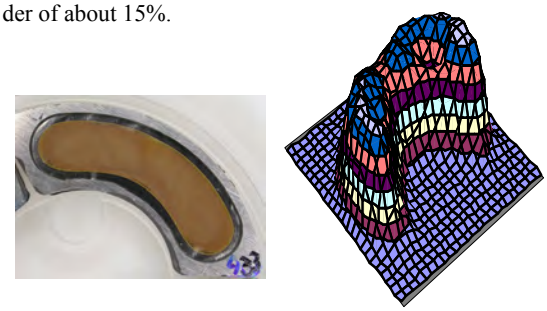

Figure 1: ^{244}Pu target segment (the brown layer indicates the Pu-oxide deposit) and corresponding plot of the activity distribution as obtained by radiographic imaging.

References

[1] Ch. E. Düllmann *et al.*, contribution to this report.
[2] A. Yakushev *et al.*, contribution to this report.
[3] J. Runke *et al.*, contribution to this report.
[4] K. Eberhardt et al., NIM A 590 (2008) 134
[5] B. Lommel et al., NIM A 590 (2008) 141
[6] D. Liebe et al., NIM A 590 (2008) 145

Recovery of ^{244}Pu from irradiated targets for production of element 114*

J. Runke[1,#], K. Eberhardt[1], J. V. Kratz[1], Ch. E. Düllmann[2] and M. Schädel[2]
[1]Institut für Kernchemie, Johannes Gutenberg-Universität Mainz, Germany; [2]GSI, Darmstadt, Germany

The ^{244}Pu targets [1] (PuO_2 electrodeposited on Ti backing) were irradiated during recent bombardments with $^{48}Ca^{10+}$ ions to produce $^{288,\ 289}$114 [2,3]. During these bombardments with up to 3.6 x 10^{18} ions, targets and backings underwent changes that made reprocessing and production of new targets for forthcoming experiments desirable.

Figure 1: Teflon vessel.

Recovery of ^{244}Pu from one arc-shaped segment was accomplished as follows: The Al-target frame was inserted into a Teflon vessel containing a cavity into which the frame could be inserted, see Figure 1. With a sharp knife, the target was cut out of the frame, the frame was removed, and the target together with the Ti backing was dissolved in hot conc. HCl. The dissolution of the Ti backing was incomplete. The central part of the backing that had received the highest beam intensity did not dissolve. The resulting solution with the remainder of the undissolved Ti was evaporated to near dryness, transferred into a 10 ml measuring flask and filled with 8 M HCl. An aliquot of that solution was removed, evaporated to dryness, and the α-particle activity was determined. The total activity was used for yield determination. The results indicate that more than 80 % of the Pu had been recovered.

*Sponsored in the frame of a GSI R&D project (MZJVKR).
runke@uni-mainz.de

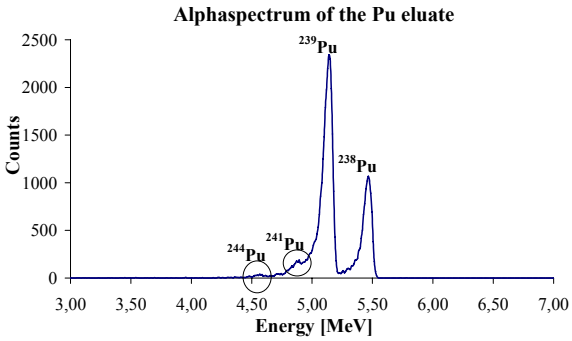

Figure 2: Alphaspectrum of the Pu eluate.

The Pu/Ti solution in 8 M HCl was transferred to a AG 1x8 anion-exchange column (3 x 50 mm), and was washed subsequently with 10 x 1 ml of 8 M HCl to remove the Ti and the ^{241}Am from the column. Then, the Pu was eluted from the column in 8 x 1 ml of 0.5 M HCl. Figure 2 shows the spectrum of α particles of an aliquot of the eluate. Due to the isotopic composition of the plutonium (97.9 % ^{244}Pu, 1.3 % ^{242}Pu, 0.7 % ^{240}Pu, < 0.1% other), the main α activities are associated with ^{238}Pu and ^{239}Pu. 100 µl of that solution was removed, filled up to 2 ml and was irradiated with thermal neutrons in the TRIGA reactor at the Institute of Nuclear Chemistry at the University of Mainz at 100 kW together with a second reference sample containing 9.62 µg ^{244}Pu for 6 h. After a decay time of 18 h, both samples were assayed for the 327.6 keV γ-activity of ^{245}Pu at a Ge detector, see Figure 3. The activation analysis showed a ^{244}Pu recovery of 89 %.

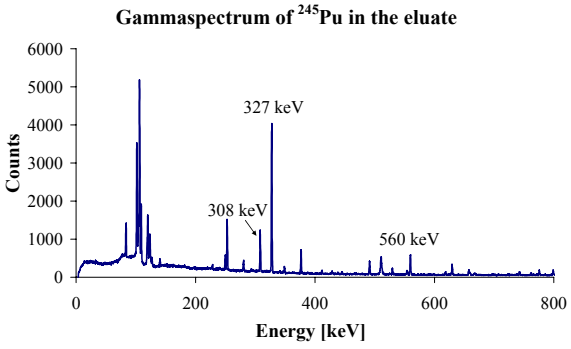

Figure 3: Gammaspectrum of ^{245}Pu solution.

References

[1] K. Eberhardt *et al.*, contribution to this report.
[2] Ch. E. Düllmann *et al.*, contribution to this report.
[3] A. Yakushev *et al.*, contribution to this report.

Theoretical Investigations of Trends in Volatility of the Heaviest Elements

V. Pershina[1], A. Borschevsky[2], J. Anton[3], and T. Jacob[3]
[1]GSI, Darmstadt, Germany; [2]School of Chemistry, Tel Aviv University, Israel; [3]Institut für Elektrochemie, Universität Ulm, Germany

Elements 112 through 118 are expected to be very volatile. Early extrapolations of the sublimation enthalpies, $\Delta H_{sub}=\Delta H_f(g)$, of the solid state in groups 12 through 17 have indeed shown the lowest ΔH_{sub} for the heaviest elements in each group of the elements, respectively [1,2]. (The gas-phase chemistry experiments give ΔH_{sub} as a measure of volatility of an element using measured ΔH_{ads} on metal surfaces and an assumed linear correlation between these values [3]). The reason for the high volatility is strong relativistic effects on the valence electrons of these elements.

It was also recognized that linear extrapolations of properties within the chemical groups should be made cautiously due to increasing (non-linearly with Z) relativistic effects. Thus, relativistic calculations are nowadays a must for reliable predictions of properties of the heaviest elements. Since ΔH_{sub} should be related to the interaction energy of an atom with itself, we have performed a systematic calculations of the M-M dissociation energies (D_e) for the entire 6p and 7p rows of the elements and compared them with the known values of $D_e(M_2)$ and ΔH_{sub} in groups 13 through 18.

For the calculations of the electronic structures of M_2 (M = Hg/112, Tl/113, Pb/114, Bi/115, Po/116, At/117, Rn/118), we have used our 4*c*-DFT method [4] proven to be a reliable tool in predicting binding energies and bond lengths. Very large optimized basis sets were used including 5g virtual atomic orbitals. Results of the calculations are summarized in Table 1.

Table 1. Optimized bond lengths R_e (in Å) and dissociation energies D_e (in eV) in M_2 (M = Tl/113 through Rn/118)

M_2	R_e	D_e	M_2	R_e	D_e
Tl_2	3.185 3.00*	0.47 0.42*	$(113)_2$	3.613	0.06
Pb_2	2.97 2.93*	1.18 1.17*;0.83*	$(114)_2$	3.49	0.13
Bi_2	2.685 2.6596*	2.23 2.05*	$(115)_2$	3.072	0.82
Po_2	2.813 -	2.15 1.94*	$(116)_2$	3.238	1.34
At_2	3.041 -	1.02 0.87±1.3*	$(117)_2$	3.524	0.77
Rn_2	-	unbound	$(118)_2$	4.498	0.012

* Experimental values; $R_e(Tl_2)$ is questionable.

Good agreement with experiment was obtained for the lighter homologs of the heaviest elements. The Rn dimer was obtained unbound, so that calculations with even larger basis sets could follow.

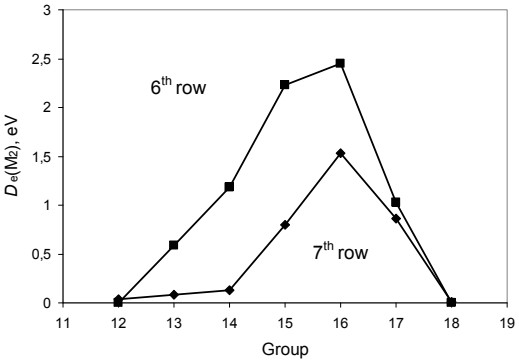

Figure 1: Calculated binding energies in group 12 through 18 homonuclear dimers.

Fig. 1 shows that $D_e[M_2]$ of the 7p elements are much smaller than $D_e[M_2]$ of the 6p homologs in groups 13 through 16. This is due to the fact that bonding in the lighter M_2 is due to the participation of both the $np_{1/2}$ and $np_{3/2}$ AOs, while the contribution of the former one is drastically diminished in the heaviest homologs (it practically forms a closed-shell). A remarkable fact is that the difference in D_e between the 6th and 7th row elements diminishes with the group number from group 15 on and gets even reversed in group 18: thus, element 118 is stronger bound to itself than Rn.

A good correlation between $D_e(M_2)$ and $\Delta H_f(g)$ was found for groups 13 through 17. On their basis, the following ΔH_{sub} for the heaviest elements were obtained: 145 kJ/mol for element 113, 70 kJ/mol for element 114, 164 kJ/mol for element 115, 101 kJ/mol for element 116, and 92 kJ/mol for element 117. These values are close to those obtained via linear extrapolations of $\Delta H_f(g)$ in the groups [1,2]. Extensive cluster calculations should be performed to confirm the predicted values.

References

[1] O.L. Keller *et al*. J. Phys. Chem. 74, 1127 (1970); *ibid*, 78 (1974) 1945.
[2] B. Eichler, Kernenergie, 10 (1976) 307.
[3] B. Eichler, R. Eichler, In: "The Chemistry of Superheavy Elements", Kluwer, 2003, Ed. M. Schädel, p. 205.
[4] J. Anton, B. Fricke, E. Engel, Phys. Rev. A, 69 (2004) 012505.
[5] H. Rossbach and B. Eichler, Akademie der Wissenschaft der DDR, Report No. ZFK-527, 1984.

Theoretical Investigations of Trends in Adsorption of the Heaviest Elements on Gold

V. Pershina[1], A. Borschevsky[2], J. Anton[3], and T. Jacob[3]
[1]GSI, Darmstadt, Germany; [2]School of Chemistry, Tel Aviv University, Israel; [3]Institut für Elektrochemie, Universität Ulm, Germany

Elements 112 through 118 are expected to be very volatile due to strong relativistic effects on their valence electrons. Their volatility is to be studied via the gas-phase thermochromatography technique by measuring the adsorption enthalpy, ΔH_{ads}, on gold plated detectors located along the chromatography column (see results for elements 112 and 114 [1,2]). The obtained ΔH_{ads} is then related to the sublimation enthalpy, ΔH_{sub}, of macroamounts using a linear correlation between these values [1].

Results of our extended cluster calculations [3] have shown that ΔH_{ads} of group 12 and 14 atoms M adsorbed on gold surface can reliably be predicted on the basis of knowledge of binding energies (D_e) of gold dimers, MAu: the difference in $D_e(M\text{-}Au_n)$, where $1 \le n \le 120$, between the adatoms M is kept almost constant independently of the gold cluster size and adsorption position. Accordingly, in this work, we try to estimate ΔH_{ads} of the 7p elements and their 6p homologs, as well as trends in the chemical rows, on the basis of the calculated D_e(MAu), where M = Tl/113, Pb/114, Bi/115, Po/116, At/117, Rn/118.

The calculations were performed with the use of our fully relativistic 4*c*-DFT method [4] proven to be a reliable tool in predicting binding energies and bond lengths. Very large optimized basis sets including 5g virtual AOs were used. Results of the calculations of the bond lengths (R_e) and D_e are summarized in Table 1.

Table 1. Optimized bond lengths R_e (in Å) and dissociation energies D_e (in eV) in MAu (M = Hg/112 through Rn/118)

MAu	R_e	D_e	MAu	R_e	D_e
HgAu	2.67	0.06	112Au	2.73	0.51
TlAu	2.668	2.72	113Au	2.716	1.83
PbAu	2.64	2.15	114Au	2.88	0.73
BiAu	2.638	2.43	115Au	2.892	2.44
PoAu	2.631	2.29	116Au	2.867	2.17
AtAu	2.644	1.97	117Au	2.835	1.87
RnAu	3.023	0.23	118Au	3.003	0.66

The calculated D_e are depicted in Fig. 1 together with the measured $-\Delta H_{ads}$ of Hg, Tl and Pb on gold; $-\Delta H_{ads}$ of element 112 (measured [1]) and 4*c*-DFT predicted for elements 113 and 114 [3]; as well as the calculated $-\Delta H_{ads}$ for Hg through Po and for elements 112 through 116 using semi-empirical models [5]. The obtained D_e(MAu) indicate that there should be no decrease in the binding energies with gold from Bi to element 115, and a very little decrease from Po and At to elements 116 and 117, respectively. Moreover, the trend in D_e gets reversed for RnAu and 118Au, in line with the expected higher reactivity of element 118 in comparison with Rn. Thus, taking into account our experience for groups 12 - 14 [3], one can expect that $-\Delta H_{ads}$ of Bi through Rn and elements 115 through 118 should follow the trends found for the D_e(MAu) of these elements (Fig. 1).

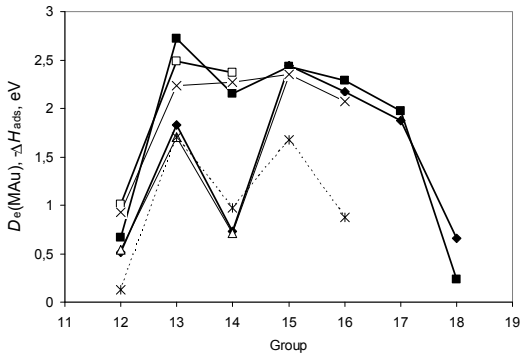

Figure 1: Binding energies: filled squares – calculated here D_e(MAu) (M = Hg through Rn), and filled rhomboids – D_e(MAu) (M = elements 112 through 118); open squares – measured $-\Delta H_{ads}$ of Hg, Tl and Pb on gold; open triangles - $-\Delta H_{ads}$ of element 112 (measured [1]) and elements 113 and 114 (4*c*-DFT predicted [3]); crosses – calculated $-\Delta H_{ads}$ for Hg through Po, and stars – for elements 112 through 116 [5].

The expected high $-\Delta H_{ads}$ of elements 115 through 117 are in contrast with the results of the semi-empirical calculations [5]: the latter show a decrease in $-\Delta H_{ads}$ from the 6p to 7p elements in groups 15 – 17, similar to that in groups 13 and 14. The present results also mean that the linear correlation between $-\Delta H_{ads}$ and ΔH_{sub} used in [1] is questionable: the estimated (via a linear extrapolation in the groups) ΔH_{sub} of elements 115 - 117 [6] are much smaller than ΔH_{sub} of Bi through At. Extensive cluster calculations are needed to confirm these conclusions.

References

[1] R. Eichler, *et al*. Nature, Letters, 447 (2007) 72.
[2] A. Yakushev, Presentation at the 7th Workshop on the Chemistry of the Heaviest Elements, Mainz, 2009.
[3] V. Pershina, J. Anton, T. Jacob, J. Chem. Phys. 131 (2009) 084713.
[4] J. Anton, *et al.,* Phys. Rev. A, 69 (2004) 012505.
[5] H. Rossbach and B. Eichler, Akademie der Wissenschaft der DDR, Report No. ZFK-527, 1984.
[6] B. Eichler, Kernenergie, 10 (1976) 307.

Theoretical Investigations of Chemical Reactivity of Element 113

J. Anton[1], V. Pershina[2] and T. Jacob[1]
[1]Institut für Elektrochemie, Universität Ulm, Germany; [2]GSI, Darmstadt, Germany

The heaviest element identified chemically is Z=112. Using the gas-phase thermochromatography technique, its volatility, i.e., the adsorption enthalpy, ΔH_{ads}, on gold plated detectors located along the chromatography column was investigated and compared to that of Hg [1]. Very recently, results of the first chemical studies on element 114 using the same technique were reported [2,3]. Both elements, 112 and 114, were shown to be very volatile which is explained by their closed, $7s^2 6d^{10}$, and quasi-closed, $7s^2 7p_{1/2}^2$, shells, respectively. Element 113 (having the $7s^2 7p_{1/2}$ ground state) is to be studied next. It is expected to be also volatile and relatively inert, though less than 112 and 114, due to the relativistic stabilization of the 7s and $7p_{1/2}$ electrons. Feasibility experiments have already been conducted for its lighter homolog, Tl [4]

Earlier, we have predicted ΔH_{ads} of elements 112 and 114 on inert and gold surfaces by performing 4c-DFT calculations for the atoms adsorbed on very large gold clusters [5]. We have also predicted ΔH_{ads} of element 113 on inert surfaces using result of accurate *ab initio* Dirac-Coulomb atomic calculations [6]. It was shown that element 113 should be well transported through the Teflon capillaries from the target chamber to the chemistry setup.

In this work, we study reactivity of element 113 and Tl on the basis of the calculations for their M_2 and MAu dimers: it was shown that binding energies in MAu are directly related to ΔH_{ads} of M on gold [5]. In addition, we study the stability of hydroxides that can be formed in the oxygen atmosphere over the gold surface.

For the calculations, we have used our 4c-DFT method [7]. Very large optimized basis sets were used. Results of the calculations for M_2, MAu and MOH (M = Tl and element 113) are given in Table 1 [9].

Table 1. Optimized bond lengths R_e (in Å), dissociation energies D_e (in eV) and vibrational frequencies w_e (in cm^{-1}) for M_2, MAu and MOH (M = Tl and element 113)

Molecule	R_e	D_e	w_e
Tl_2	3.185	0.479	67
$(113)_2$	3.613	0.058	25
TlAu	2.668	2.669	141
113Au	2.716	1.825	144
TlOH	2.176	3.680[a]	547
113OH	2.282	2.424[a]	519

[a] with respect to the MOH = M + OH decomposition

The potential energy curves for TlAu and 113Au are shown in Fig. 1. One can see a decrease in D_e of 0.84 eV from TlAu to 113Au with a respective bond lengthening of 0.048 Å, similar to that of Tl_2 with respect to $(113)_2$ (of 0.42 eV), and that of the simple hydrides and fluorides of these elements, found in other calculations.

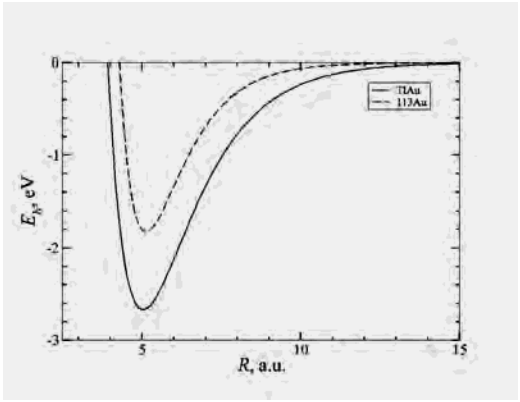

Figure 1: Calculated binding energies in TlAu and 113Au.

Using the difference in D_e between MAu and 113Au, one can estimate $-\Delta H_{ads}(113)$ on a gold surface with respect to the measured $-\Delta H_{ads}(Tl)$ = 240 ± 5 kJ/mol [4]. Thus, one can expect that element 113 will adsorb on gold at about 0.84 eV (82 kJ/mol) lower energies than Tl. This gives a preliminary value of $\Delta H_{ads}(113)$ = -158.6 kJ/mol, which is very close to -164.4 kJ/mol predicted with the use of adsorption models and extrapolation of properties in group 13 [8]. According to the results, the sequence in the volatility of the heaviest elements should be 112 > 114 > 113.

The data of Table 1 also indicate that the M-OH bonds should be stronger and shorter than the M-Au ones. This explains why Tl reacts preferentially with OH and not with gold in the oxygen atmosphere. The same is expected for element 113 forming a stronger 113-OH bond than the 113-Au one. The $-\Delta H_{ads}$(113OH) on gold is expected to be lower than $-\Delta H_{ads}(113)$.

References

[1] R. Eichler *et al.* Nature, Letters, 447 (2007) 72.
[2] R. Eichler, Abstract of the NRC7 International Conference, Budapest, 24-29 August 2008.
[3] A. Yakushev, Presentation at the 7th Workshop on the Chemistry of the Heaviest Elements, Mainz, 2009.
[4] S. König, *et al*., PSI Annual Report 2005, 2006, p. 5.
[5] V. Pershina, J. Anton, T. Jacob, J. Chem. Phys. 131 (2009) 084713.
[6] V. Pershina, A. Borschevsky, E. Eliav, U. Kaldor, J. Phys. Chem. A 112 (2008) 13712.
[7] J. Anton, *et al*., Phys. Rev. A, 69 (2004) 012505.
[8] H. Rossbach and B. Eichler, Akademie der Wissenschaft der DDR, Report No. ZFK-527, 1984.
[9] V. Pershina, J. Anton, T. Jacob, Chem. Phys. Lett. 480 (2009) 157.

Electron Affinity of Element 114, with Comparison to Sn and Pb

A. Borschevsky[1], V. Pershina[2], E. Eliav[1], and U. Kaldor[1]
[1] School of Chemistry, Tel Aviv University, Israel; [2] GSI, Darmstadt, Germany

Knowledge of the electronic structure and properties of element 114 is important for its chemical identification. By comparing its behaviour with that of the lighter group 14 homologues, its position in the periodic table can be confirmed.

In this work, we investigate the electron affinity (EA) of element 114, together with its lighter homologues in group 14, Sn and Pb [1]. Electron affinity is important for calculations of chemical potential, μ, and electronegativity, χ, which, in turn, reflect chemical reactivity of the element under study.

The calculations were performed in the framework of the projected Dirac-Coulomb-Breit Hamiltonian,

$$H_{DCB} = \sum_i h_D + \sum_{i<j} (1/r_{ij} + B_{ij}), \quad (1)$$

where

$$h_D = c\vec{\alpha}\cdot\vec{p} + \beta c^2 + V_{nuc}\,. \quad (2)$$

Here, V_{nuc} is the nuclear attraction operator, and α and β are the four-dimensional Dirac matrices. The nuclear potential, V_{nuc}, takes into account the finite size of the nucleus, modelled as a uniformly charged sphere. The two electron terms include the nonrelativistic electron repulsion and the Breit term, B_{ij}, and are correct to the second order in the fine structure constant.

Electron correlation is taken into account using the Fock space (FS) [2] and mixed sector intermediate Hamiltonian (MSIH) [3] coupled cluster (CC) methods, which are considered to be one of the most powerful tools in quantum chemistry.

Two types of the basis sets were used in the calculations, that of Faegri [4] and the even tempered universal basis set of Malli *et al*. [5]. For each of the elements under study, both types of the basis sets were extended to convergence. The size of the model spaces used was gradually increased in order to obtain convergence of the results.

The calculated electron affinities of Sn and Pb are shown and compared with experiment [6] in Table 1.

Table 1. Electron affinities of Sn, Pb, and element 114 (in meV).

Method	Sn		Pb		Element 114	
	I	II	I	II	I	II
FSCC	736	735	247	245	No EA	No EA
MSIH	1085	1072	383	363	No EA	No EA
Exp. [6]	1112		364			

I- Faegri basis set; II – Malli basis set.

The FSCC EA values are about 35% too low, while the MSIH results are within 5% of the experiment. This is due to the possibility of employing large and flexible model spaces within the MSIH framework. Good agreement with experiment, as well as the very small differences between the results for the two types of the basis sets, confirm the convergence of the MSIH calculations.

The same methods were used to estimate the electron affinity of element 114. All the calculations have given negative electron affinities. Thus, the very good agreement of the MSIH EAs of Pb and Sn, and the converged exhaustive calculations for element 114, lead to the conclusion that element 114 will not bind an extra electron.

This prediction is in accord with the trend in the EAs of group 14 elements. The EAs of the group 14 elements go down monotonically, as is shown in Fig. 1. The decrease is enhanced for Pb by the relativistic destabilization of the $6p_{1/2}$ orbital. As is shown by the dashed line in Figure 1, an extrapolation of the line from Sn to Pb crosses the *x* axis well before Z=114. In fact, an even steeper decrease may be expected for element 114, which should exhibit stronger relativistic effects than Pb. This supports our prediction that no electron binding will occur in element 114.

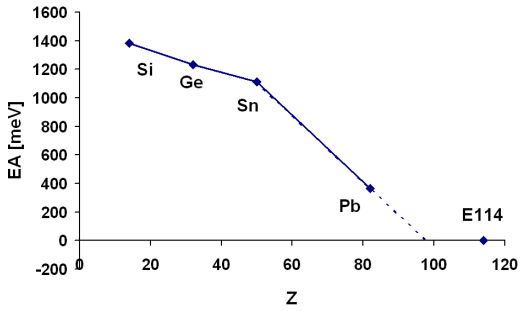

Fig. 1. Electron affinities of group 14 elements. The dashed line is an extrapolation from Sn and Pb.

References

[1] A. Borschevsky, V. Pershina, E. Eliav, and U. Kaldor. Chem. Phys. Lett. 480 (2009) 49.
[2] E. Eliav, U. Kaldor, and Y. Ishikawa, Phys. Rev. A 49 (1994) 1724.
[3] A. Landau, E. Eliav, Y. Ishikawa, and U. Kaldor, J. Chem. Phys. 121 (2004) 6634.
[4] K. Faegri, Theor. Chim. Acta 105 (2001) 252.
[5] G.L. Malli, A.B.F. Da Silva, Y. Ishikawa, Phys. Rev. A 47 (1993) 143.
[6] H. Hotop, W.C. Lineberger, J. Phys. Chem. Ref. Data 4 (1975) 539, *ibid*, 14 (1985) 731.